

INVESTIGATIONS OF THE PARK COOL ISLAND EFFECT
OF GOLDEN GATE PARK, SAN FRANCISCO

A thesis submitted to the faculty of
San Francisco State University
In partial fulfillment of
The Requirements for
The Degree

Master of Science
In
Geographic Information Science

by

Stephanie May Cowles

San Francisco, CA

January, 2014

CERTIFICATION OF APPROVAL

I certify that I have read Title of Thesis/Title of Dissertation by Stephanie May Cowles, and that in my opinion this work meets the criteria for approving a thesis submitted in partial fulfillment of the requirements for the degree: Master of Science in Geographic Information Science at San Francisco State University.

Andrew Oliphant
Professor of Geography

Jerry Davis
Professor of Geography

Investigations of the Park Cool Island Effect of Golden Gate Park, San Francisco

Stephanie May Cowles
San Francisco, CA
2014

The cooling effect of urban green spaces, termed the "park cool island" (PCI) is touted for energy savings and as a mitigation for heat waves, which are expected to increase in frequency and severity as a result of climate change. The variability and complexity of the Golden Gate Park cool island in San Francisco, CA is explored using bicycle transects of near-surface temperature profiles from six fine-wire thermocouples mounted between 0.15 and 2.5 m above the surface. Transects were measured over different surfaces including city streets at varying distance downwind of the park as well as short grassy meadows and a grove of coastal redwood trees within the park. Long-term meteorological station data inside and nearby the park provide regional context. Surface temperature profiles varied significantly from super-adiabatic lapse rates over street surfaces to isothermal conditions in the redwood grove. A significant daytime PCI effect with mean 1.1°C in the grassy meadow and 1.8°C in the redwood grove was evident, which increased to 2.5°C in the meadow and 3.5°C in the grove under heat wave conditions. The vertical temperature gradient was greatest within 0.15 m of the surface, while the horizontal gradient between park and urban surroundings dissipated within 500 m of the park. Temperature characteristics within the park varied significantly with surface cover and patterns of sun and shade. PCI intensity was related to overall temperature and absolute humidity within the park. Results suggest that the cooling effect of Golden Gate Park, while persistent, is not a significant source of cooling outside the park. However, vertical profile measurements are a promising method that could provide a baseline for assessing the impact of planned urban greening interventions such as green roofs, street trees, and permeable pavement on the near-surface thermal environment in cities.

I certify that the Abstract is a correct representation of the contents of this thesis.

Chair, Thesis Committee

Date

ACKNOWLEDGEMENT

This work would not have been possible without the dedicated efforts of Professor Andrew Oliphant, chair of my thesis committee, who has been available and involved throughout. I'd also like to thank Professor Jerry Davis, for reading drafts and providing valuable critiques, Caitlin Jensen and David Prigge for helping with data collection, and Sarah Harling, for support throughout and consultation on map design. I'd also like to thank the faculty of the San Francisco State University Geography Department and my fellow graduate students for fostering an environment of collaboration and mutual support.

TABLE OF CONTENTS

1. Introduction	1
2. Materials and Methods.....	5
2.1 Study Area	6
2.2 Mobile Transects	8
2.2.1 Mobile Transect Routes	8
2.2.2. Instrument Design.....	10
2.3 Fixed Station Data	14
3. Results.....	15
3.1 Afternoon Vertical Temperature Profiles	17
3.2 Park Cool Island Effect.....	20
3.3 Role of Shade in Park Cooling	22
3.4 Humidity as an indicator of Park Cooling.....	27
3.5 Park to Urban Temperature Gradient.....	31
4. Discussion.....	34
4.1 Afternoon Vertical Temperature Profiles	34
4.2 Park Cool Island Effect.....	35
4.3 Role of Shade in Park Cooling	37
4.4 Humidity as an indicator of Park Cooling.....	38
4.5 Park to Urban Gradient	40
5. Conclusions	41
6. Works Cited.....	43

LIST OF TABLES

Table 1. Date, time of day and weather type for mobile transects along longitudinal and land cover routes through Golden Gate Park and vicinity.	12
Table 2. Mean PCI (μ_{PCI}) and standard deviation (σ_{PCI}) in Sharon Meadow and Memorial Grove at each measurement height. Sample size (n) and number of unique days represented in the samples are also listed. The small sample sizes for elevated heat days may be a source of error.	22
Table 3. The relationship between vapor pressure and mean PCI for (a) combined measurements in both park land cover areas, (b) Memorial Grove only, and (c) Sharon Meadow only. The relationship was significant in each case ($p < 0.001$). Linear regression on sample size (n) was used to calculate the rate of change in temperature per kPa as well as the model fit (r^2 value).	27
Table 4. Relationship between humidity and mean PCI intensity in Sharon Meadow and Memorial Grove under typical and elevated heat weather conditions.....	30
Table 5. Temperature gradient between the park and Kirkham transect routes, and rate of temperature change with distance from the ocean on longitudinal profile routes through Golden Gate Park and along Kirkham Street as measured from the temperature probe mounted at 0.5 m a.g.l. Routes are mapped in Figure 1.	31
Table 6. Change in temperature between Sharon Meadow and Block 3, a distance of 1.01 km, for all transects with no missing values for measurement heights or sampled land cover area (n=18). The shaded values fall within the range of the onshore gradients calculated in Table 5.....	32

LIST OF FIGURES

- Figure 1. Sampled land cover areas and longitudinal transect routes in and around Golden Gate Park, San Francisco, CA (37.77°N, 122.48°W, elevation ~ 30 m).6
- Figure 2. San Francisco Peninsula and San Francisco Bay, including the Golden Gate Park and locations of stationary measurement sites.7
- Figure 3. Maximum and minimum daily temperatures in Downtown San Francisco and Oceanside. Dotted lines represent transect days. Source: National Climatic Data Center (NCDC, ncdc.noaa.gov). See Figure 2 for locations.16
- Figure 4. (a) Temperature (b) wind speed and (c) relative humidity before, during and after the heat event of September 30 to October 2, 2013 as measured from the rooftop of the Cal Academy. See Figure 1 for the location of the measurement site in the context of the study area and Figure 2 for the site in regional context.17
- Figure 5. Average temperature profile for each sampled land cover area across three late afternoon transects in Golden Gate Park and vicinity.18
- Figure 6. Box-whisker plots for each sampled land cover area showing the distribution of the mean difference between the instantaneous temperature measurement at each height and the mean temperature across all measurement heights during afternoon transects. At each measurement height, the box represents the 25th to 75th percentile temperature difference. The median is represented as a vertical line. The tails of the distribution are represented as the horizontal whiskers. The points represent outliers. Block 2 is omitted: the pattern is indistinguishable from Blocks 1 and 3. Measurement heights are shown categorically and are not to scale.19
- Figure 7. Average profile of PCI intensity in Memorial Grove and Sharon Meadow from four transects during October 14, 2012.21
- Figure 8. Mean PCI intensity (μ_{PCI}) at each measurement height for Sharon Meadow and Memorial Grove under typical and elevated heat conditions. The error bars around the mean represent one standard deviation (σ_{PCI}) in each direction. Due to sensor failure, no measurements were available at 0.15 m a.g.l. in Sharon Meadow during the elevated heat period. All available transect measurements were used in these calculations. Sample sizes are listed in Table 2.21

Figure 9. Thirty-second moving average of temperature at each measurement height and surface radiometric temperatures (at measurement height zero) measured during late afternoon transect route on October 14, 2012. Shading represents shade en route determined by one second measurements of incoming solar radiation less than 100 Wm^{-1}23

Figure 10. Five second moving average time-series of temperature profiles (a) at midday in Memorial Grove, (b) at midday in the mixed-deciduous grove, (c) at midday in Sharon Meadow, and (d) in late afternoon in the meadow on September 30. The meadows in c and d were half in shadow and were sampled up to approximately 200 seconds in the sunlit section with the remainder in the shaded section.....24

Figure 11. Distribution of temperature gradients (Eq. 2) across all transects and times of day in each sampled land cover area within 0.5 m a.g.l. Shaded circles indicate the temperature gradient for each one-second sample and are shaded according to incident solar radiation. The circles are distributed evenly across the width of each plot for clarity. Mean and standard deviation of gradients is shown above each sampled land cover area.....26

Figure 12. Mean temperature at each measurement height from transects conducted on the (a) morning and (b) early afternoon of October 2, under conditions of unusually high heat and recent irrigation. Lowest thermocouple malfunctioned for transects in (b).....28

Figure 13. Mean temperature at each measurement height from transects conducted on the morning and early afternoon of October 14, under morning fog conditions and condensation on the ground.29

Figure 14. Relationship between mean PCI intensity and the ratio of absolute humidity in Block 3, furthest from the park, and park areas at 0.5 m above ground level. Vapor pressure was calculated based on the mean relative humidity and mean temperature at 0.5 m in each sampled land cover area.....30

Figure 15. Temperature gradients during the heat event and under typical conditions between Sharon Meadow and Block 1, Block 2, and Block 3 for each transect where mean temperature measurements at 1.1 m a.g.l. were available.33

1. Introduction

Urban areas are typically warmer than the surrounding suburban or rural areas, due primarily to differences in land cover types and surface materials. This is known as the urban heat island effect. By contrast, urban green spaces account for most of the variation in temperature across cities (Gomez et al 1998, Hart and Sailor 2008, Yokobori and Ohta 2009, Lindén 2011, Murphy et al 2011, Sun 2011). Persistently cooler green spaces within urban heat islands, described as park cool islands (PCI), have been confirmed experimentally across climate types, including: dry-summer and humid subtropical, tropical, warm- and hot-summer continental, arid, semi-arid, maritime temperate, and dry-winter temperate (Bowler et al. 2010). When urban temperatures increase, the daytime temperature in parks with moderate tree coverage increases more slowly than the surrounding urban environment, offering potential relief to urban dwellers (Cohen 2012, Shashua-Bar and Hoffman 2000). Green spaces have long been proposed as a mitigation strategy for urban heat islands (Givoni 1991, Rosenfeld 1995). Increasingly, the cooling effects of urban green spaces are a critical component of urban planning particularly for climate change (Bowler et al. 2010).

PCI intensity, defined as $PCI = T_u - T_p$ where T_p is the temperature within the park and T_u is the temperature of the urban surroundings has been used as a quantifier of the magnitude of the cooling effect of parks. Repeated studies over four decades of surface temperature contrasts (Yu and Hein 2006; Cao et al. 2010; Lu et al. 2012) and air temperature contrasts (summarized in a meta-study by Bowler et al. 2010) have confirmed the existence of park cool islands across climate types and seasonal and

diurnal conditions. Daytime park cooling is primarily a function of two factors that alter the surface energy balance: shade, which decreases the net incoming solar radiation, and evapotranspiration, which shifts the partitioning of incoming solar energy from sensible heat to latent heat of evaporation. There are other factors that elevate urban heat, including heat from combustion (Shashua-Bar and Hoffman 2000; Hart and Sailor 2008), and other factors that affect cooling, especially ventilation and urban geometry. Nighttime park cooling is produced by a different set of factors, most significantly that after sunset, vegetated surfaces cool much more rapidly than asphalt, concrete and other building materials with a high heat storage capacity, widening the gap in surface temperature between parks and the surroundings throughout the night (Souch and Grimmond 2005). Heat storage can account for up to 50% of net energy balance above urban surfaces, much of which is reradiated after dark (Grimmond and Oke 1999).

The concept of PCI may suggest continuity in spatial and temporal patterns of temperature across urban parks, distinguishing the park climate from the surrounding urban area, however this continuity is not borne out empirically. It is possible to demonstrate that a single tree can reduce air temperature beneath its canopy by over 2°C (Rosenfeld 1995; Streiling and Matzarakis 2003), however variations in vegetative structure, urban geometry, and patterns of sun and shade make the signal of that cooling difficult to trace with distance from the tree, particularly in daytime amidst other turbulent flows (Yokohari et al. 1997, Ca et al. 1998, Chang et al. 2007). For this reason, empirical studies of “park breezes” typically rely on nighttime stillness to demonstrate that pressure gradients between the cooler park air and warmer urban air can lead to weak circulations that advect cool air radially out of the park (Eliasson and Upmanis 2000). During the day, when the atmosphere is actively heating, the park is not

necessarily cooler near its center (Upmanis et. al 1998). The heterogeneous configurations of vegetation and other park surface types, with different levels of cultivation and irrigation are likely to produce heterogeneous microclimates within the park, with internal boundary layers that interact thermodynamically both within parks and across park-urban boundaries.

Temperature contrasts across urban and park spaces have most commonly been studied at uniform heights: either by comparing air temperature 1 to 3 m above ground level (a.g.l.) within the park and outside of it (Yokohari 2001), or by using thermal imagery and thermography to demonstrate the contrast in surface temperatures between vegetated surfaces and the surrounding asphalt, metal, and concrete. Although contrasting surface temperatures are related to contrasting air temperatures, air temperature and “skin” temperature measured from thermal imaging are separate phenomena (Heisler and Brasel 2010). PCI intensity is smaller in magnitude when measured from air temperature than when measuring surface temperatures as thermal energy diffuses slowly through the laminar sub-layer of air directly above or adjacent the surface (Oke 1987). The timing of the maxima and minima are less predictable because the air temperature is a product of turbulent mixing of nearby microclimates (Spronken-Smith and Oke 1998).

While examining PCI along a horizontal plane above the surface is useful for establishing that park cool islands occur across regions and urban climate types, with comparable diurnal and seasonal cycles, it is less useful for characterizing the internal dynamics of park cool islands, or the mixing between boundary layers around the edges of the park. Estimating the effect of an urban park on the surrounding area based on

stationary measurements at uniform heights can lead to incomplete comprehension of the underlying mechanisms and variables. In the current study, rather than measuring park cooling at a single height or from stationary sites, vertical temperature structure in the lowest 2.5 m was recorded via mobile sampling to better account for the dynamic mixing of air masses at different scales.

The current study seeks to investigate park cooling in San Francisco, California, a coastal Mediterranean climate typically influenced by a well-developed sea breeze system. Saaroni et al. (2000) found near-surface temperatures in coastal urban areas were strongly correlated with exposure to sea breeze and that park-urban contrasts persist primarily in areas sheltered from the sea breeze. Ocean cooling can be particularly pronounced in summer, when sea breezes in Mediterranean climates are typically stronger due to the strengthening of onshore pressure gradients. For example Gomez et al. (1998) observed a pronounced winter park cool island, but no measurable park cool island in summer in Valencia, Spain.

The objective of this study is to evaluate spatial variability in vertical temperature structure near the surface within Golden Gate Park and the surrounding urban environment of San Francisco, CA during the summer. In particular, the study aims to elucidate, not only the magnitude and structure of the PCI but the spatial variability within the park associated with land surface type, humidity and shade. In addition, the diurnal variability and role of synoptic conditions on the PCI will be explored.

2. Materials and Methods

The spatial complexity of temperature and air flows in urban spaces as well as logistical challenges make siting of meteorological stations in parks difficult (Chang et al. 2007). Mobile transects averaged over a measurement area can provide a rough approximation of area-level conditions (Jauregui 1990/1991, Wong and Yu 2005, Murphy et al. 2011, Saaroni et al. 2011). A disadvantage of mobile measurements is that they do not measure different locations simultaneously and can incorporate temporal changes at the diurnal timescale into the 'spatial' results. In addition, high frequency point sampling from a mobile source can produce anomalous results due to short term fluctuations associated with turbulent motions. However, error associated with these effects can be minimized by keeping mobile transect lengths within a short enough time to assume stationarity and to obtain sufficient samples over representative surfaces of interest to average out high frequency fluctuations.

Spronken-Smith and Oke (1998) suggest that bicycles are better mobile transect vehicles than cars for park cool island studies because they reduce the contributions of car exhaust and advection from roadways, and provide better access to unpaved park interiors. For the current study, a bicycle transect method was used to obtain vertical profile measurements, adapted from Jansson et al. (2007) and Chow et al. (2011). Temperature was measured at six heights simultaneously to capture the vertical temperature structure as well as contrasts in temperatures above different land cover types. Fixed station data provided additional information about overall conditions across the study period.

2.1 Study Area

Golden Gate Park (37.77°N, 122.48°W, elevation 30 m) is a large (422 ha) urban green space in western San Francisco, sloping gently downward across 5 km between central San Francisco to the east and the Pacific Ocean to the west, with a width of 0.9 km (Figure 1). Based on land cover classification using LiDAR elevation data and 1 m resolution orthoimagery, approximately 62% of the park is forested. An additional 10% is short grass, primarily meadows, playing fields and a golf course and 2% is other types of vegetation. The remaining 16% is comprised of buildings, parking lots, roadways and other impervious surfaces.

The park is surrounded by medium density residential neighborhoods. Based on the 2010 US Census, the population density within one kilometer of Golden Gate Park is 74 people per hectare. Whereas 74% of Golden Gate Park is vegetated, 13% of the area of urban neighborhoods within 1 km of Golden Gate Park are vegetated. Since Golden Gate Park is west of the major topographic barriers in San Francisco, it is among the least sheltered from wind and advection fog.

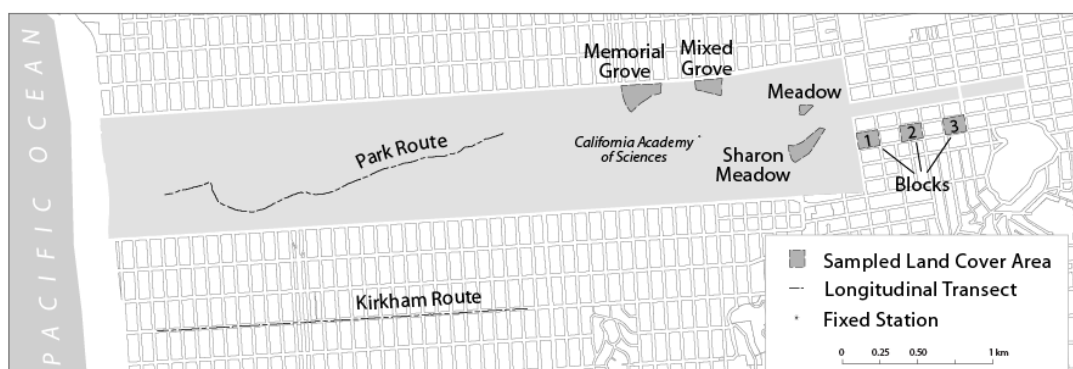


Figure 1. Sampled land cover areas and longitudinal transect routes in and around Golden Gate Park, San Francisco, CA (37.77°N, 122.48°W, elevation ~ 30 m).

The San Francisco Bay Area (Figure 2) has a Mediterranean climate with moderate temperatures year-round and consistent winds from the west/northwest. It is generally classified as Csb in the Köppen climate classification system, a cooler Mediterranean climate with maximum daily temperatures in summer rarely exceeding 25°C or falling below 5°C in winter, and scant rainfall between June and October. The average maximum daily temperature between 1995 and 2010 was 17.8°C. Temperatures are moderated by the ocean, and in particular by exposure to the sea breeze and advection fog. The sea breeze is strongest in the afternoon starting around 3 pm and persisting well after sunset. Elevation ranges from sea level to around 450 m along the two branches of the California Coastal range, which runs north-south on either side of the Bay, bisecting San Francisco and the urbanized areas of the East Bay. Proximity to the ocean and topography largely determine which areas are more exposed to fog and sea breeze.



Figure 2. San Francisco Peninsula and San Francisco Bay, including the Golden Gate Park and locations of stationary measurement sites.

Seasonally, fog and strong sea breezes are most common in the summer months, between June and August, when the cold coastal California Current is strongest. This induces strong temperature gradients between surface water and air, and between sea and land. Conversely, the highest annual temperatures typically occur during late spring or early autumn as heat events that are synoptically distinct from typical conditions: the North Pacific Ocean high pressure system ridges eastward inland over the Pacific Northwest, bringing warm and dry NE air-masses into Northern California.

2.2 Mobile Transects

2.2.1 Mobile Transect Routes

A mobile transect was conducted 27 times through eastern Golden Gate Park and urban areas southeast of the park sampling the five areas shown in Figure 1: Sharon Meadow, a cultivated grassy playing field near the eastern entrance to the park, the World War I Memorial Grove north of the De Young Museum and the California Academy of Sciences (Cal Academy), and three city blocks, spaced 300 m apart from each other and centered 450, 750 and 1,010 m from the eastern edge of the park between Haight Street and Page Street south of the Panhandle. The areas are all comparable in size: the city blocks are each 1.5 ha in area, Sharon Meadow is 2.1 ha, and Memorial Grove is 2.9 ha overall, but only the eastern 1.5 ha was sampled. Sharon Meadow is edged with trees and man-made features, but open to the sky. Conversely Memorial Grove is a very dense redwood grove, with limited light penetration except

along a wide path at the northern edge. Most of the streets bounding the city blocks are 18 to 24 m wide, uniformly lined by adjoined three story buildings, and sparse tree canopies. Masonic Street is 30 m wide, with higher traffic speeds and volumes are high, and traffic on Haight Street is moderate and slow. Traffic on all other sides of the city blocks is light.

During each transect, approximately 200 to 300 one-second samples were logged over 2.5 to 3 minutes in each of the five study locations. Observations about meteorological conditions were recorded at the end of each transect, along with records of whether the park areas had been recently irrigated. According to the San Francisco Recreation and Parks Department, turf areas in Golden Gate Park are irrigated 1-3 times per week during the dry season between May and November (personal communication, May 22, 2013). During heat events, they are irrigated more frequently to protect the plants from the biophysical impacts of heat. Memorial Grove is primarily irrigated only during extensive dry periods. Irrigation was observed in Memorial Grove on August 8 and 9 and September 12 and 13.

Two additional sites indicated in Figure 1 were sampled on September 30 to characterize the role of shade in producing park cooling: a meadow north of the primary field (Meadow 2, ~ 0.4 ha) and a mixed deciduous grove of trees west of the primary grove with a clearing and picnic tables in the center (~ 1.5 ha).

Two longitudinal transects were conducted on July 5 and July 31 along routes that ran from midway through Golden Gate Park to the Pacific Ocean (Figure 1). The routes were approximately 1 km apart (range: 0.75 m to 1.1 m, mean distance: 0.9). These transects were intended to distinguish park cooling from any west to east temperature

gradient associated with the sea breeze. The urban route ran along Kirkham Street, which runs parallel to the park at a distance of ~ 0.64 km to the south. Kirkham is a wide street with very little shade three blocks from the park. The route through the middle of the park was along park roads and a paved trail, mostly in shade with patches of sun. Both longitudinal transects were conducted under typical summer weather conditions. Conditions on July 5 were mostly sunny, with cool temperatures and a moderate breeze coming from the northwest. Conditions on July 31 were overcast with fog increasing toward the Pacific coast.

2.2.2. Instrument Design

Bicycles were fitted with Omega Type E fine wire thermocouples (diameter .076 mm) mounted at six levels on a 2.5 m tall rubber-sheathed aluminum pole. Six different heights were chosen after testing to best represent the structure of the observed vertical temperature profiles: 0.15 m, 0.3 m, 0.5 m, 0.7 m, 1.1 m and 2.5 m above ground level (a.s.l). A LiCor190SB Quantum Sensor was mounted on the top of the pole to record incoming solar radiation (wavelength 0.4 to 0.7 μm), and a HMP45C probe shaded under the logger box recorded air temperature and relative humidity. Thermocouples were unshielded, since tests confirmed that direct sunlight did not impact the measurements. All measurements were logged at one second intervals on a Campbell Scientific CR1000 data logger that was mounted on the front of the bike in a reflective weather-proof box with insulation to maintain a stable data logger temperature which was used as a reference for the thermocouple measurements. For transects on October 14, 2012, an

Apogee thermal infrared radiometer was mounted facing forward to record surface radiometric temperatures. Latitude and longitude were recorded at one-second intervals using a Trimble Juno SB handheld GPS unit mounted on the front of the bike. Synchronization of the clocks on the logger and GPS were verified to the second at the beginning of each transect.

Temperature, relative humidity, and solar radiation measurements were combined with latitude and longitude using customized Python scripts and ArcGIS 10.0 for each one second observation. On the few occasions where the GPS lost contact with satellites and failed to record any location information, observations from within sampled land cover areas were identified from manual logs of entrance and exit times.

To protect against loss and breakage, twelve thermocouples were calibrated for the six slots against a recently factory-calibrated Vaisala HMP60 thermistor. The instruments were co-located on a mast 2 m above the rooftop of a building on the San Francisco State University campus for the period of a week. Sensors were sampled at one-second intervals and averaged every five minutes, providing a sample size of 1,981. Linear regression slopes between each thermocouple and the reference thermistor ranged between 0.99 and 1.01 and r^2 values were all greater than 0.975. The mean standard deviation between the thermocouples was 0.12°C and this variation showed no bias (mean bias error was $2.5 \cdot 10^{-17}$). We could therefore conclude that differences observed between the thermocouples during transects were almost entirely due to physical differences rather than instrumentation differences. In a few cases thermocouples were damaged during bicycle transects and data from damaged sensors were removed from analysis.

Tests were also conducted to compare observations recorded when travelling in the windward direction to those recorded in the downwind direction due to effects of the bicycle or rider on the measurements. The temperatures were not affected at any height. Post-processing of the data confirmed that travel speeds were relatively consistent at 2 m s⁻¹, excluding stop signs and stop lights. Observations were removed where the travel speed was less than 0.2 m s⁻¹.

Table 1 shows the general weather conditions and timing of transects throughout the study period. Transects were generally conducted in the afternoon. Extra transects were conducted during the heat event to assess park cooling over the diurnal cycle. Transects on September 30 and October 2 were conducted during an extreme heat event as defined by the California Energy Commission (<http://cal-adapt.org/>): daytime temperatures exceeded the 98th percentile of normal maximum temperatures. The event brought the warmest temperatures of the study period and of 2012.

Table 1. Date, time of day and weather type for mobile transects along longitudinal and land cover routes though Golden Gate Park and vicinity.

	Morning / Dawn	Early Afternoon	Late Afternoon	Dusk
2012-05-07			☀️☁️	
2012-12-07		☀️☁️		
2012-24-07			☀️	
2012-31-07			☁️☀️	
2012-08-08			☀️☁️	
2012-09-08		☁️☀️		
2012-14-08			☀️☁️	
2012-25-08			☀️☁️	
2012-28-08			☁️	
2012-12-09		☁️	☁️	
2012-13-09	☁️		☀️☁️	
2012-23-09		☀️☁️	☀️☁️	
2012-30-09		☀️🌡️	☀️🌡️	☀️🌡️
2012-02-10	☀️🌡️	☀️🌡️	☀️🌡️	☀️🌡️
2012-03-10		☀️		
2012-14-10	☁️	☁️☀️	☀️	☁️☀️

☀️ Sunny
☀️🌡️ Elevated heat
☀️☁️ Mostly sunny
☁️☀️ Partly cloudy
☁️ Clouds/fog

The contrast between maximum temperature and daily temperature ranges in Downtown San Francisco and Oceanside throughout the study period illustrates the strong temperature contrasts from the coast to central city. The daily minimum temperatures are quite similar across the city but the afternoon maxima are strongly limited to the west by the marine air advecting onshore. Assuming the maxima occurred around the same time, the gradient between the maxima with distance from the ocean between the two stations averaged $0.45^{\circ}\text{C km}^{-1}$ (range: -0.1 to $1.9^{\circ}\text{C km}^{-1}$). The temperature spike between September 30 and October 2 represents the heat event, and the maximum temperature gradient of $1.9^{\circ}\text{C km}^{-1}$. The higher than average temperatures were precipitated by a synoptic-scale change in weather patterns.

The contrast between maximum temperature and daily temperature ranges in Downtown San Francisco and Oceanside throughout the study period illustrates the strong temperature contrasts from the coast to central city, just 8.4 km away. The Downtown station is located 6.9 km further from the ocean than the Oceanside station. The daily minimum temperatures are quite similar across the city but the afternoon maxima are strongly limited to the west by the marine air advecting onshore. Assuming the maxima occurred around the same time, the gradient between the maxima with distance from the ocean between the two stations averaged $0.45^{\circ}\text{C km}^{-1}$ (range: -0.1 to $1.9^{\circ}\text{C km}^{-1}$). The temperature spike between September 30 and October 2 represents the heat event, and the maximum temperature gradient of $1.9^{\circ}\text{C km}^{-1}$. The higher than average temperatures were precipitated by a synoptic-scale change in weather patterns.

In total seven (7) transects were conducted during the elevated heat period: three (3) on September 30 and four (4) October 2. Four transects were conducted on October

14 to measure the progression of park cooling throughout a more typical summer day. The thermocouple sensors at 0.15 m failed on July 31 and all four transects on October 2. The thermocouple at 2.5 m failed on September 13. Elevated temperatures recorded at the logger box on July 5 suggested the box was improperly shielded from solar radiation, thus thermocouple measurements from this transect were not used. Overall, 12 transects were conducted in early afternoon, 11 in the late afternoon, 2 at dawn, 1 in the morning and 3 in the evening. Transects took between 30 and 40 minutes with a median duration of 35 minutes. Temperatures at the fixed station above the California Academy of Sciences building in Golden Gate Park changed by less than $\pm 0.3^{\circ}\text{C}$ during these intervals and wind speed was below 4 m s^{-1} 95% of the time.

2.3 Fixed Station Data

Wind speed and temperature observations averaged at 5 minute intervals were obtained from above the green roof on the California Academy of Sciences (Cal Academy) building in Golden Gate Park, 3.9 km from the Pacific Ocean (elevation 75 m, building height 14 m). The green roof is planted with perennial native plants and wildflowers less than 10 cm tall, with a soil depth of 3-5 cm. Three domes built into the roof surround a piazza that is opened at night to cool the interior of the building through cold air drainage, which may artificially increase nighttime rooftop temperatures. The instrumentation is sited approximately 2 m above the southeast corner of the roof. Distance from building edges and other obstructions that might cause updrafts or downdrafts were evaluated at the site before the observational data was obtained.

Daily temperature minima and maxima obtained from the National Climatic Data Center (NCDC, ncdc.noaa.gov) through the Global Historical Climatology Network provide temperature ranges across San Francisco overall during the study period. The locations of the stations, in Downtown San Francisco on South Van Ness Avenue, and Oceanside at the San Francisco Zoo, are shown in Figure 2. The Downtown station is 6.9 km further from the ocean than the Oceanside station.

3. Results

The contrast between maximum temperature and daily temperature ranges in Downtown San Francisco and Oceanside throughout the study period illustrates the strong temperature contrasts from the coast to central city. The daily minimum temperatures are quite similar across the city but the afternoon maxima are strongly limited to the west by the marine air advecting onshore. Assuming the maxima occurred around the same time, the gradient between the maxima with distance from the ocean between the two stations averaged $0.45^{\circ}\text{C km}^{-1}$ (range: -0.1 to $1.9^{\circ}\text{C km}^{-1}$). The temperature spike between September 30 and October 2 represents the heat event, and the maximum temperature gradient of $1.9^{\circ}\text{C km}^{-1}$. The higher than average temperatures were precipitated by a synoptic-scale change in weather patterns.

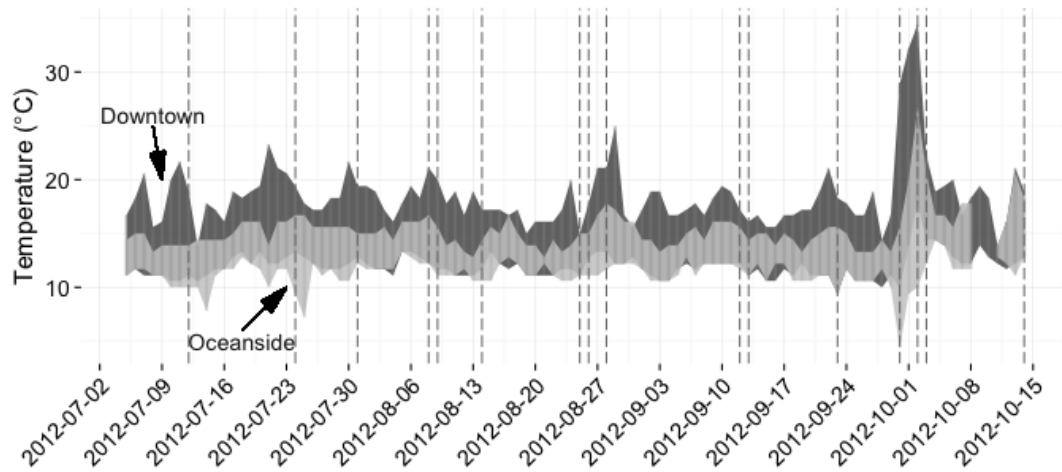


Figure 3. Maximum and minimum daily temperatures in Downtown San Francisco and Oceanside. Dotted lines represent transect days. Source: National Climatic Data Center (NCDC, ncdc.noaa.gov). See Figure 2 for locations.

The influence of typical maritime conditions was disrupted by a continental high pressure system marked by clear skies, low wind, and a sharp decrease in relative humidity (Figure 4). During the heat event, the sea breeze pattern of winds peaking around mid-afternoon was diminished and air temperatures remained near their noontime peak until after 4 pm. The days preceding and following the heat event show the more typical pattern in San Francisco, with moderate sea breezes attenuating afternoon temperatures and raising humidity.

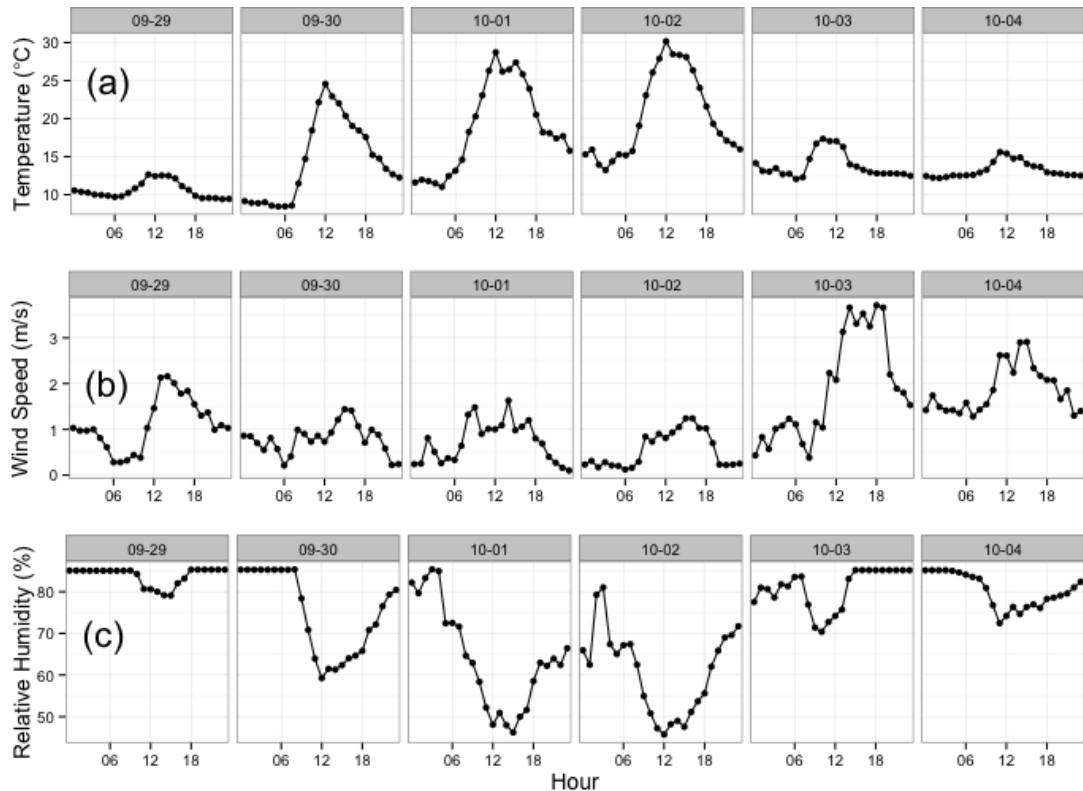


Figure 4. (a) Temperature (b) wind speed and (c) relative humidity before, during and after the heat event of September 30 to October 2, 2013 as measured from the rooftop of the Cal Academy. See Figure 1 for the location of the measurement site in the context of the study area and Figure 2 for the site in regional context.

3.1 Afternoon Vertical Temperature Profiles

Vertical temperature profiles shown in Figure 5 demonstrate the characteristic similarities and differences between each of the sampled land cover areas in the afternoon under typical cool summer conditions. Blocks 1, 2 and 3 did not vary significantly in vertical profiles or mean temperatures and show a strong lapse to about 0.5 m with isothermal conditions above to 2.5 m. Sharon Meadow and Memorial Grove were significantly different from the city blocks both in mean temperature and

temperature structure and were also significantly different from each other. Memorial Grove was consistently the coolest and was nearly isothermal at all times of day. Sharon Meadow was consistently cooler than the city blocks and warmer than Memorial Grove, yet had the steepest near-surface lapse. In fact, on about half of the early afternoon transects, Sharon Meadow was as warm, and on two occasions warmer, than the city blocks at 0.15 m a.g.l.

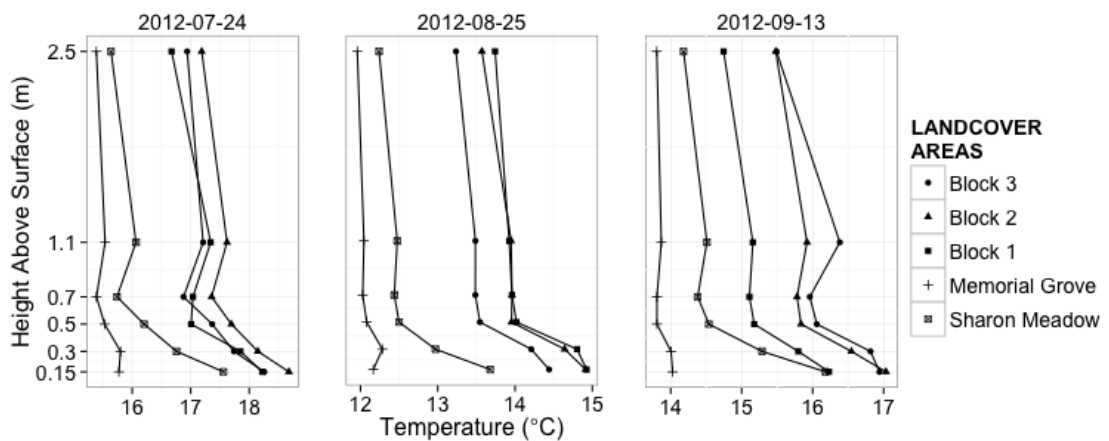


Figure 5. Average temperature profile for each sampled land cover area across three late afternoon transects in Golden Gate Park and vicinity.

Within blocks, observations were classified by street segment orientation to further test whether the street grid was producing localized microclimates based on sun and wind exposure. There was no significant difference in temperature between streets oriented north-south and streets oriented east-west.

Figure 5 also shows a small inversion layer that was commonly observed between about 0.3 and 1.1 m a.g.l. and occurred in all sampled land cover areas. This micro-inversion was visible to some degree on all afternoon transects under elevated heat and typical conditions except for a cloudy late afternoon transect on September 12, and was less prominent or not evident in transects in the morning or at dusk.

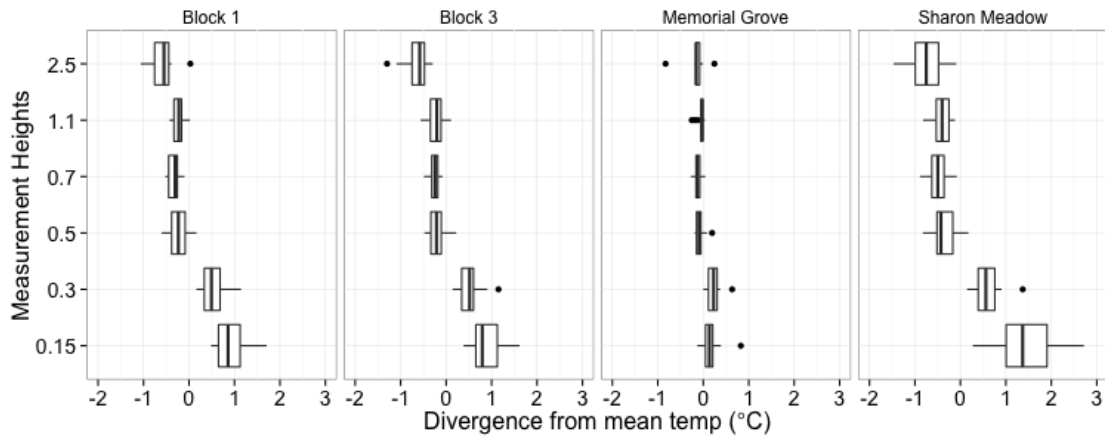


Figure 6. Box-whisker plots for each sampled land cover area showing the distribution of the mean difference between the instantaneous temperature measurement at each height and the mean temperature across all measurement heights during afternoon transects. At each measurement height, the box represents the 25th to 75th percentile temperature difference. The median is represented as a vertical line. The tails of the distribution are represented as the horizontal whiskers. The points represent outliers. Block 2 is omitted: the pattern is indistinguishable from Blocks 1 and 3. Measurement heights are shown categorically and are not to scale.

Figure 6 demonstrates that each sampled land cover area had a characteristic late afternoon profile that persisted from day to day. The temperature measurements at each height were most variable at 0.15 m a.g.l., and were especially variable in Sharon Meadow. By contrast, Memorial Grove is the most consistent and nearly isothermal. Blocks 1, 2 (not shown) and 3 were similar in the distribution of mean temperature differences at each measurement height, just as they were similar in temperature and temperature structure overall. When the temperature at each height was normalized by mean temperature (Figure 6), evidence of the inversion layer noted in specific transects (Figure 5) disappeared. Temperature contrasts between park areas and the surrounding urban blocks are discussed in greater detail in the next section.

3.2 Park Cool Island Effect

Mean PCI intensity was defined as,

$$\mu_{\text{PCI}} = T_{\text{Block 3}} - T_{\text{Park}} \quad (1)$$

Where $T_{\text{Block 3}}$ is the temperature around Block 3, approximately 1,010 m from the park, T_{Park} is the temperature in Sharon Meadow or Memorial Grove, and n is the total number of transects used to calculate the mean. Under typical summer conditions, afternoon mean PCI intensity at 1.1 m a.g.l. was 1.1°C in Sharon Meadow and 2.0°C in Memorial Grove. The mean PCI intensity for Sharon Meadow and Memorial Grove under typical conditions across all measurement heights and times of day was 1.5°C whereas under elevated heat conditions it was 3.2°C, more than twice as large.

Figure 7 shows how PCI varied throughout the course of a typical summer day, and the contrast in the magnitude of park cooling in Sharon Meadow and Memorial Grove at different measurement heights. In the morning, PCI was very near zero in both Memorial Grove and Sharon Meadow. By afternoon, as temperatures increased, PCI intensity in Memorial Grove increased to between 1.2 and 1.9°C, significantly greater than PCI intensity in Sharon Meadow, where the effect size was -1.6°C near the surface and approaching zero with height above the surface. In the late afternoon, PCI intensity in Sharon Meadow increased at all measurement heights, while PCI intensity in Memorial Grove remained unchanged. At dusk, PCI had diminished considerably, however PCI intensity in Memorial Grove and Sharon Meadow converged, and both remained higher directly above the surface.

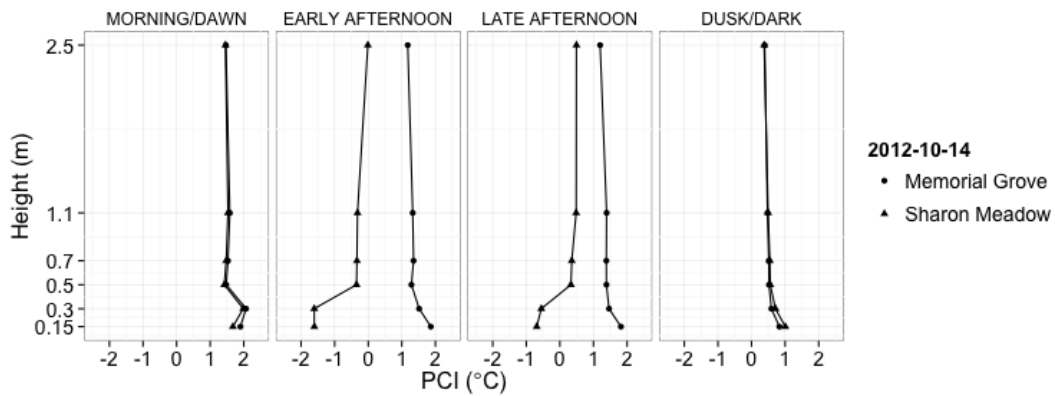


Figure 7. Average profile of PCI intensity in Memorial Grove and Sharon Meadow from four transects during October 14, 2012.

Figure 8 shows how mean PCI intensity varies with height in the surface layer overall, and that mean PCI intensity nearly doubled under elevated heat conditions relative to typical cool conditions. In Memorial Grove, the change in PCI intensity with height is similar under typical and elevated heat conditions, despite an overall difference in mean PCI intensity of more than 1.5°C : mean PCI intensity is greatest at the surface, and decreases by 0.6°C under typical conditions and by 0.8°C under elevated heat conditions at 0.5 m a.g.l.

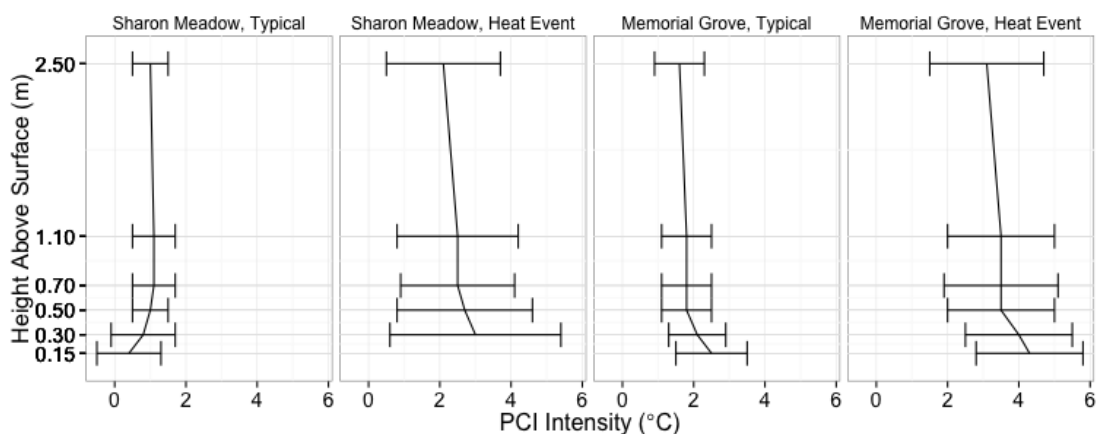


Figure 8. Mean PCI intensity (μ_{PCI}) at each measurement height for Sharon Meadow and Memorial Grove under typical and elevated heat conditions. The error bars around the mean represent one standard deviation (σ_{PCI}) in each direction. Due to sensor failure, no measurements were available at 0.15 m a.g.l. in Sharon Meadow during the elevated heat period. All available transect measurements were used in these calculations. Sample sizes are listed in Table 2.

The mean PCI intensities at each measurement height in typical and elevated heat conditions are listed in Table 2 along with standard deviations and sample size differences for each measurement. The inversion evidenced in Sharon Meadow during the elevated heat period is based entirely on transect measurements made on October 2, 2012. Irrigation the previous day may explain why the shape of the vertical profile differs from the curve based on typical conditions, as explored in Section 3.4.

Table 2. Mean PCI (μ_{PCI}) and standard deviation (σ_{PCI}) in Sharon Meadow and Memorial Grove at each measurement height. Sample size (n) and number of unique days represented in the samples are also listed. The small sample sizes for elevated heat days may be a source of error.

	Height (m)	Overall				Sharon Meadow				Memorial Grove			
		μ_{PCI}	σ_{PCI}	N	days	μ_{PCI}	σ_{PCI}	n	days	μ_{PCI}	σ_{PCI}	n	days
Typical	0.15	1.5	1.4	30	11	0.4	0.9	16	11	2.5	1.0	16	11
	0.3	1.5	1.2	32	11	0.8	0.9	16	11	2.1	0.8	16	11
	0.5	1.4	0.7	32	11	1.0	0.5	16	11	1.8	0.7	16	11
	0.7	1.5	0.7	32	11	1.1	0.6	16	11	1.8	0.7	16	11
	1.1	1.4	0.7	32	11	1.1	0.6	16	11	1.8	0.7	16	11
	2.5	1.3	0.7	32	11	1.0	0.5	16	11	1.6	0.7	16	11
Elevated heat	0.15	4.8	1.7	5	2	n.a.	n.a.	1	1	4.3	1.5	4	2
	0.3	3.6	1.8	11	2	3.0	2.4	4	1	4.0	1.5	7	2
	0.5	3.2	1.6	11	2	2.7	1.9	4	1	3.5	1.5	7	2
	0.7	3.2	1.6	11	2	2.5	1.6	4	1	3.5	1.6	7	2
	1.1	3.1	1.6	11	2	2.5	1.7	4	1	3.5	1.5	7	2
	2.5	2.7	1.6	11	2	2.1	1.6	4	1	3.1	1.6	7	2

3.3 Role of Shade in Park Cooling

In the absence of irrigation, daytime cooling was greatest where solar radiation was blocked. Within each sampled land cover area, the greatest temperature changes occurred in shade, and the deep shade of Memorial Grove was consistently the coolest sampled land cover area overall.

Figure 9 demonstrates that within the overall temperature variability across the transect route, even small shaded areas were correlated with decreased temperature at

all measurement heights, though more strongly for air temperature nearer the surface and by far most strongly for surface radiometric temperature, which was only measured on October 14.

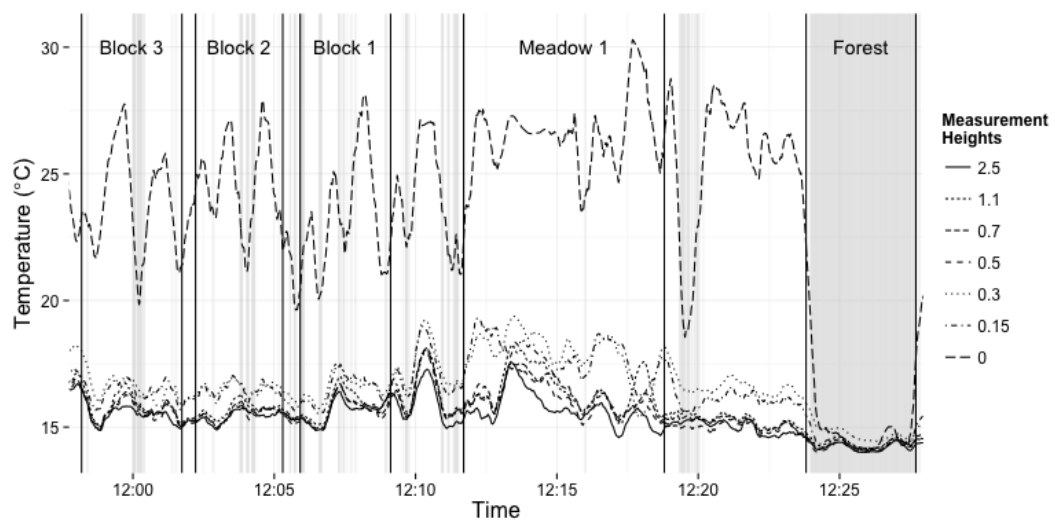


Figure 9. Thirty-second moving average of temperature at each measurement height and surface radiometric temperatures (at measurement height zero) measured during late afternoon transect route on October 14, 2012. Shading represents shade en route determined by one second measurements of incoming solar radiation less than 100 Wm^{-1} .

The correlation between shade and temperature, and measurement height and variability, were consistent across all transects. This pattern was stronger under sunny weather conditions. Temperature was highest and the most variable at the surface, with both temperature and variability decreasing with height. The thick shaded band in Figure 9 represents measurements in Memorial Grove, when temperatures were at their lowest, including surface temperature, which only dipped below air temperature in Memorial Grove.

Figure 10 shows the temperature structure in Memorial Grove, the mixed deciduous grove and Meadow 2 on September 30, during the elevated heat period. Figure 10 (a) compares Memorial Grove, which had limited light reaching the forest floor, with (b) the less dense mixed deciduous grove. In the mixed deciduous grove, pockets of warmth show up where solar radiation is heating the surface in canopy gaps, creating highly localized lapse conditions, surrounded by cooler air with temperature inversions. In the more dense, closed canopy of Memorial Grove, temperatures were lower overall by about 1°C and the temperature structure shows a more consistent surface inversion.

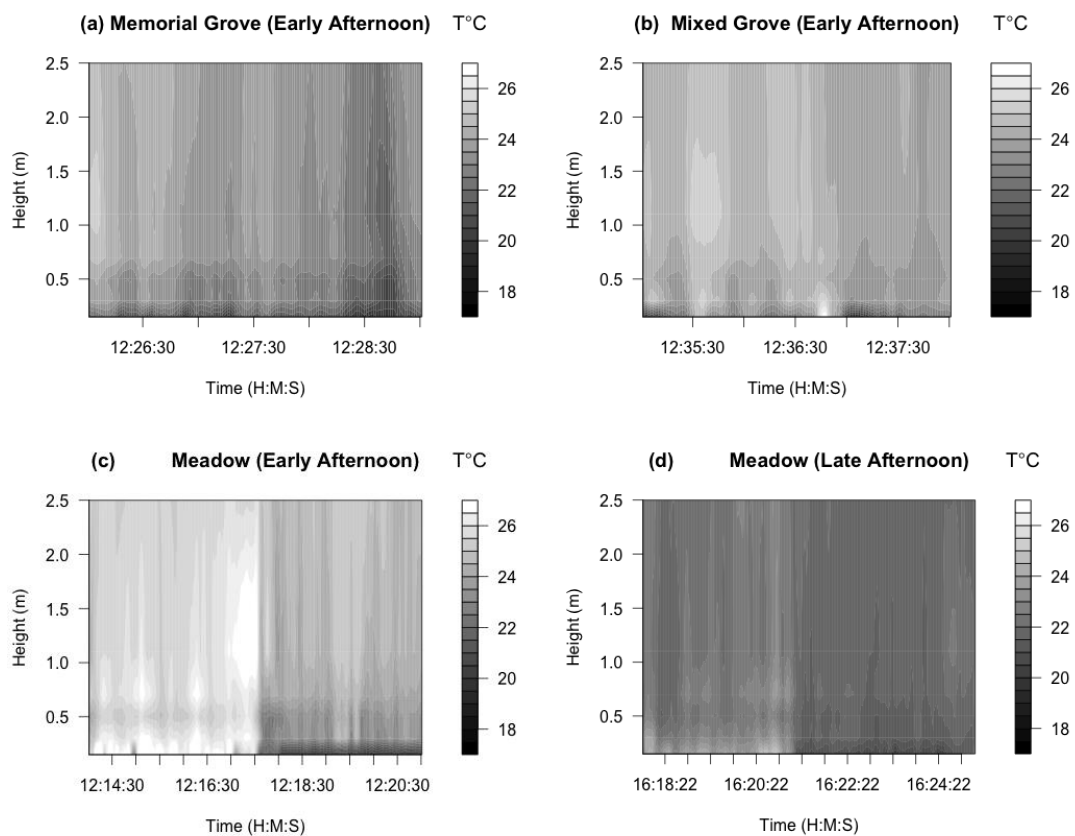


Figure 10. Five second moving average time-series of temperature profiles (a) at midday in Memorial Grove, (b) at midday in the mixed-deciduous grove, (c) at midday in Sharon Meadow, and (d) in late afternoon in the meadow on September 30. The meadows in c and d were half in shadow and were sampled up to approximately 200 seconds in the sunlit section with the remainder in the shaded section.

Meadow 2 was half in shade from surrounding trees during two transect periods, making it possible to compare shade effects in an open area with uniform surface cover (Fig. 7c and d). The sunlit section was 8°C warmer than the shaded section at 0.15 m a.g.l and 1°C warmer at 2.5 m a.g.l. at noon and only warmer by half as much (4 to 0.5°C) at 4 pm. In both cases, the sunlit section produced a surface temperature lapse, while the portions in the shade produced a surface inversion. The contrast in both mean temperature and temperature structure was clearly larger at 12 pm.

The relationship between the amount of incoming solar radiation and temperature structure was most pronounced within the lowest 0.5 m a.g.l. The temperature gradient between 0.15 and 0.5 m was calculated for each one-second sample using:

$$\frac{\Delta T}{\Delta z} = \frac{T_{0.5} - T_{0.15}}{0.35} \quad (2)$$

where $\frac{\Delta T}{\Delta z}$ is the temperature gradient (°C m⁻¹) and the subscript numbers refer to the thermocouple heights that were used.

Figure 11 shows strong contrasts in temperature gradients both characteristically between surface types and due to incident solar radiation at all sites. In general, the strongest lapses were observed when the solar radiation was highest, whereas neutral or positive temperature gradients were associated with shade.

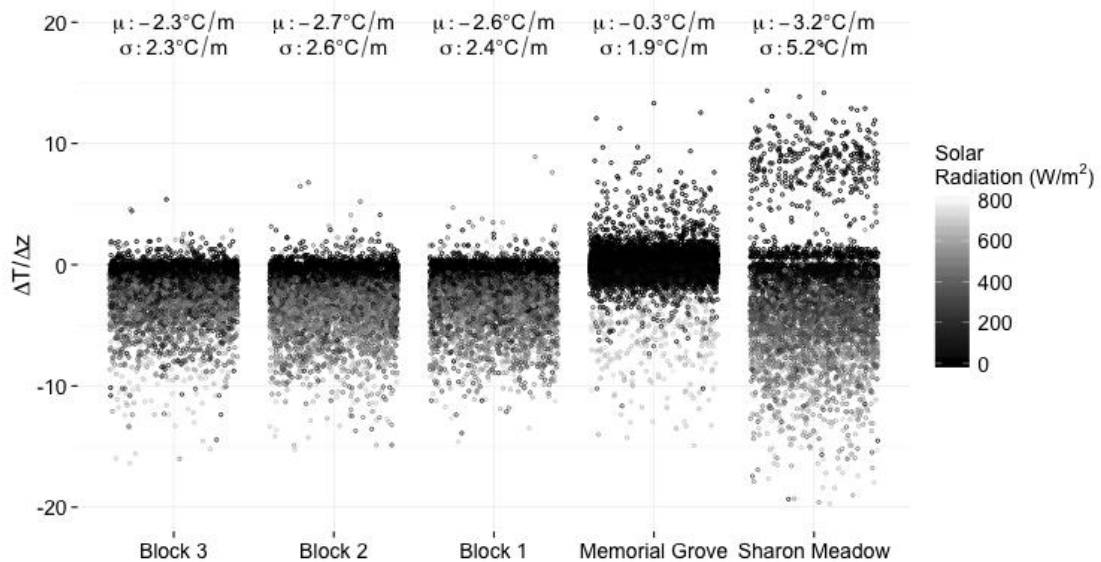


Figure 11. Distribution of temperature gradients (Eq. 2) across all transects and times of day in each sampled land cover area within 0.5 m a.g.l. Shaded circles indicate the temperature gradient for each one-second sample and are shaded according to incident solar radiation. The circles are distributed evenly across the width of each plot for clarity. Mean and standard deviation of gradients is shown above each sampled land cover area.

Inversions within 0.5 m of the surface typically only occurred in shade or low light conditions. The three city blocks were very similar to each other, seldom showing surface inversions and with lapse rates strongly correlated with insolation. In Memorial Grove the average lapse was close to neutral, but showed the largest number of surface inversion samples. With a mostly closed canopy, insolation was almost always low. The few exceptions when sunlight was able to penetrate produced the strongest lapse conditions found in this site. The range in temperature gradient was highest in Sharon Meadow, which produced the strongest lapse rates of all surface types. These rates were also correlated with insolation and low light produced either neutral or inversion conditions near the surface. This site also showed the strongest inversion rates, although these outliers were observed in the early morning of October 2 following irrigation (Section 3.3).

3.4 Humidity as an indicator of Park Cooling

Although past studies have used relative humidity as an indicator of park cooling (Jauregui 1990/1991), specific humidity or vapor pressure is more typical, since they are not temperature dependent. In the current study, vapor pressure was calculated from relative humidity in order to examine water vapor content independently. Temperature values at 0.5 m a.g.l., the approximate height of the humidity probe, were used to calculate saturated vapor pressure and test its relationship to mean PCI intensity. The results, along with sample size and model fit, are shown in Table 3. The positive correlation was significant in both Sharon Meadow and Memorial Grove, although stronger for Memorial Grove.

Table 3. The relationship between vapor pressure and mean PCI for (a) combined measurements in both park land cover areas, (b) Memorial Grove only, and (c) Sharon Meadow only. The relationship was significant in each case ($p < 0.001$). Linear regression on sample size (n) was used to calculate the rate of change in temperature per kPa as well as the model fit (r^2 value).

	<i>(a) Combined</i>			<i>(b) Memorial Grove</i>			<i>(c) Sharon Meadow</i>		
Height	$^{\circ}\text{C kPa}^{-1}$	r^2	n	$^{\circ}\text{C kPa}^{-1}$	r^2	n	$^{\circ}\text{C kPa}^{-1}$	r^2	n
0.5	0.1	0.79	29	0.13	0.86	14	0.07	0.71	13

One feature that distinguishes urban green spaces from natural vegetation is that they are frequently irrigated. In semi-arid climates and climates with a dry season such as San Francisco's, this difference can mean significantly greater water availability in urban parks compared to natural areas. Figure 12 and Figure 13 contrast the effects of irrigation on temperature with the effects of wet fog on temperature.

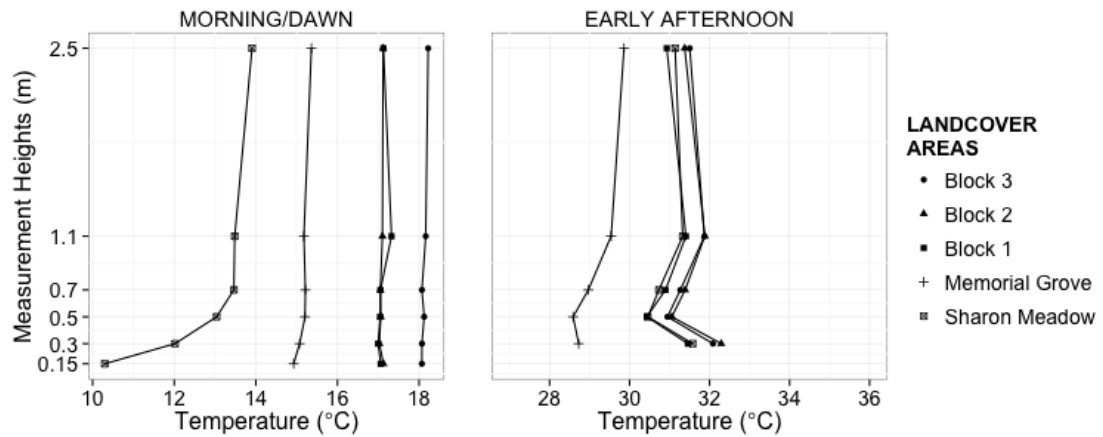


Figure 12. Mean temperature at each measurement height from transects conducted on the (a) morning and (b) early afternoon of October 2, under conditions of unusually high heat and recent irrigation. Lowest thermocouple malfunctioned for transects in (b).

Figure 12 shows a strong surface inversion to 0.7 m in Sharon Meadow after it was irrigated between the evening of September 30 and the evening of October 1, compared to the other sampled land cover areas. These measurements were taken during the elevated heat period, when the highest mean PCI intensity values were recorded and relative humidity dropped by around a third: from around 80% to around 60%, thereby increasing the evaporative potential of the atmosphere (Figure 4). This was the only transect measurement where Sharon Meadow was significantly cooler near the surface than the air above. Temperatures near the surface were up to 4.5°C cooler than Memorial Grove and 6.8°C cooler than the city blocks. Above 0.5 m a.g.l, temperatures in Sharon Meadow were 1.5°C and 3.5°C cooler than the city blocks. By noon, the effect of irrigation on the temperature profile had disappeared, and vertical profiles within Sharon Meadow mirrored the lapses of the city blocks.

In contrast, Figure 13 shows vertical temperature profiles in Sharon Meadow that were warmer than those above the city blocks. On the morning of October 14, dense advection fog covered the study area and condensation was visible on the surface. The

cooler park temperature pattern disappeared altogether with very little difference between all sites in both mean temperature and temperature profiles which were nearly isothermal. By early afternoon, the air temperature had warmed by 1-5°C across the measurement heights, although the temperature measurements closest to the surface were still lower than the overlying air temperatures across all sampled land cover areas. By late afternoon, the sky was clear, and the temperature profiles in the city blocks were not significantly different from the temperatures in Sharon Meadow, although Sharon Meadow remained slightly warmer near the surface.

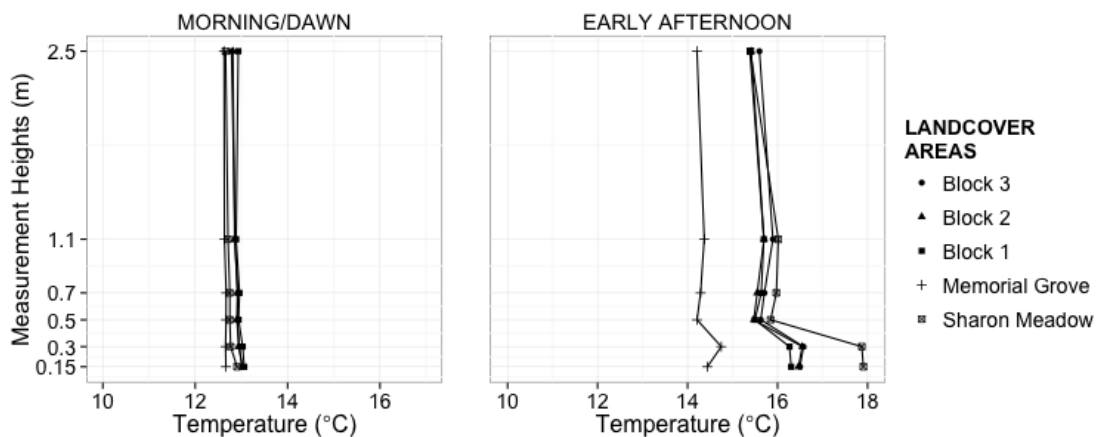


Figure 13. Mean temperature at each measurement height from transects conducted on the morning and early afternoon of October 14, under morning fog conditions and condensation on the ground.

Absolute humidity in the park correlated with mean PCI intensity as shown in Table 3, but the difference between absolute humidity inside the park and absolute humidity outside of the park is also predictive, as shown in Table 4. The relationship was consistent in all park sampled land cover areas. Overall, the difference between absolute humidity in Block 3 and absolute humidity in Sharon Meadow and Memorial Grove explained 78% of the variation in mean PCI intensities measured at 0.5 m a.g.l. across all

transects. The effect size was stronger in Memorial Grove than in Sharon Meadow, and stronger with distance from the surface.

Table 4. Relationship between humidity and mean PCI intensity in Sharon Meadow and Memorial Grove under typical and elevated heat weather conditions.

		RH, Park (%)	T, Park (°C)	RH, Block 3 (%)	Mean PCI Intensity	Absolute Humidity, Block 3 (kPa)	Absolute Humidity, Park (kPa)	Absolute Humidity, Park - Block 3 (kPa)
Elevated heat	Sharon Meadow	62.2	16.3	50	4	1.6	2.1	0.5
	Memorial Grove	70.9	16.3	50	3.7	1.4	2.1	0.7
Typical	Sharon Meadow	78	15.3	74.3	0.9	1.3	1.4	0.1
	Memorial Grove	82	14.5	74.3	1.7	1.2	1.4	0.2

Figure 14 shows the park was almost always more humid than the city blocks and that the humidity ratio was positively correlated with PCI intensity. The light grey symbols representing values from the heat event show a continuation of the linear trend under warmer, less humid conditions.

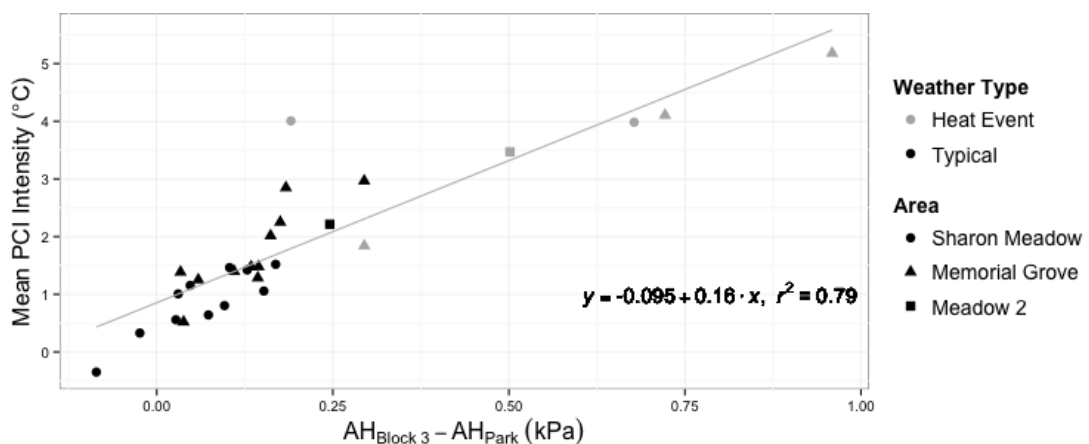


Figure 14. Relationship between mean PCI intensity and the ratio of absolute humidity in Block 3, furthest from the park, and park areas at 0.5 m above ground level. Vapor pressure was calculated based on the mean relative humidity and mean temperature at 0.5 m in each sampled land cover area.

3.5 Park to Urban Temperature Gradient

Longitudinal profiles conducted on July 5 under sunny conditions and July 31 under cloudy skies showed that the route through the park was cooler than the route along Kirkham Street (routes shown on Figure 1). However, as shown in Table 5, the temperature probe at 0.5 m showed a larger gradient under sunny conditions on July 5 than under overcast conditions on July 31, with an average difference of 4.8 and 1.4°C respectively. Over an average distance of 0.9 km, this translates to park to urban gradients of 5.3 and 1.5°C km⁻¹.

Table 5. Temperature gradient between the park and Kirkham transect routes, and rate of temperature change with distance from the ocean on longitudinal profile routes through Golden Gate Park and along Kirkham Street as measured from the temperature probe mounted at 0.5 m a.g.l. Routes are mapped in Figure 1.

	<i>Sunny (July 5, 2012) ΔT ($^{\circ}\text{C km}^{-1}$)</i>	<i>Overcast (July 31, 2012) ΔT ($^{\circ}\text{C km}^{-1}$)</i>
$T_{urban} - T_{park}$	4.8	1.4
Park to urban gradient:	5.3	1.5
<i>Onshore gradient:</i>		
Park	0.9	-0.2
Kirkham	1.2	0.6

The onshore gradient with distance from the ocean shown in Table 5 was calculated based on simple linear regression. It was greater along the Kirkham Street transect than through the park. Under overcast conditions, the onshore gradient was negligible in the park. Although the longitudinal profile measurements were taken at 0.5 m a.g.l. and the fixed station measurements presented in Section 3.1 were taken above rooftop height, the onshore gradient values presented in Table 5 are comparable to the 0.1 to 1.6°C km⁻¹ range of maximum temperatures measured at the fixed stations.

The experimental design also included three city blocks of increasing distance from the park. This was used to determine block-scale temperature gradients from the park to the surrounding urban area. These blocks were immediately to the east of the park and therefore also associated with the broader west-east temperature gradient, which had the same sign. It was estimated by taking the average of the mean difference between temperatures in Sharon Meadow and Block 3 at each thermocouple for transects with no missing values (n=18).

The shaded values in Table 6 fall between 1.2 and $-0.2^{\circ}\text{C km}^{-1}$, the range of values for the estimated onshore gradient shown in Table 5, therefore the rate of warming could be explained by increasing distance from the ocean rather than park cooling. The temperature gradient between Sharon Meadow and Block 1 was only slightly greater than the onshore gradient.

Table 6. Change in temperature between Sharon Meadow and Block 3, a distance of 1.01 km, for all transects with no missing values for measurement heights or sampled land cover area (n=18). The shaded values fall within the range of the onshore gradients calculated in Table 5.

<i>Measurement Height (m)</i>	<i>$\Delta T (^{\circ}\text{C km}^{-1})$</i>			
	Sharon Meadow to Block 1	Block 1 to Block 2	Block 2 to Block 3	Sharon Meadow to Block 3
0.15	1.0	0.7	0.4	0.7
0.3	1.9	0.6	0.7	1.1
0.5	2.1	0.6	0.8	1.2
0.7	2.1	0.6	0.9	1.3
1.1	2.1	0.4	1.0	1.2
2.5	2.0	0.3	0.9	1.2

Although the mean temperatures were increasing with distance from the park and ocean, on some individual transects the temperature was decreasing, as shown in Figure

15. Also shown in Figure 15, the gradient was stronger and more consistent during the heat event. At 0.15 m a.g.l. the gradient was most variable, and was cooler at Block 3 on 6 out of 19 transects. At measurement heights above 0.3 m, the only increasing temperature gradient occurred on October 14 during the early afternoon transect profiled in Figure 7.

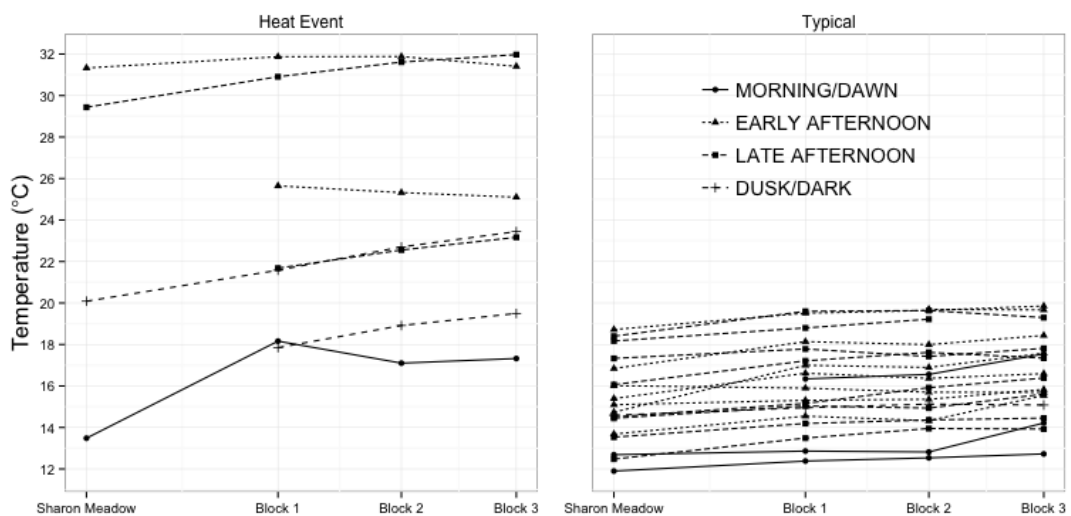


Figure 15. Temperature gradients during the heat event and under typical conditions between Sharon Meadow and Block 1, Block 2, and Block 3 for each transect where mean temperature measurements at 1.1 m a.g.l. were available.

4. Discussion

4.1 Afternoon Vertical Temperature Profiles

The similarity between temperatures near the surface in Sharon Meadow and the city blocks reinforces the findings of Cao et al. (2010) based on measurements from thermal satellite imagery that grass parks do not produce park cooling. Spronken-Smith and Oke (1998) found that temperatures near the surface of mowed grass produce a midday lapse similar to the lapse observed in Sharon Meadow. The openness of Sharon Meadow means the surface is more consistently exposed to solar radiation, which is absorbed and reradiated throughout the day. The openness could also mean greater exposure to sea breezes (Saaroni et al. 2000), which would allow cooler air from aloft to increase the temperature lapse rate at the surface in Sharon Meadow. The absence of street canyon walls, which tend to reradiate absorbed solar radiation from vertical as well as horizontal surfaces, may also partially explain why Sharon Meadow is cooler than the city blocks overall (Voogt and Oke 1997).

The isothermal temperature profiles in Memorial Grove are likely a result of the fact that the trees greatly reduce sunlight from reaching the surface. Instead, solar radiation is primarily absorbed in the upper canopy of the trees, and surface heating is driven by longwave radiation absorption from the surrounding trees. It is likely therefore to produce a temperature inversion near the top of the canopy, which was 20-30 m above the lowest 2.5 m of the atmosphere measured in this study. With limited undergrowth, these measurements were made in relatively open trunk space, allowing mixing within

this layer, which would also support the production of an isothermal profile near the surface. The results confirm findings from past studies that forested areas are cooler than non-forested urban areas during the day (Wong and Yu 2005; Yu and Hein 2006; Hart and Sailer 2009).

Finally the consistency of vertical profile patterns around city blocks suggests the mobile sampling technique sufficiently resolved the difficulty noted in past studies of finding representative reference points in urban environments, despite the uneven patterns of insolation and ventilation across urban street grids (Chang et al. 2007). However since there was no significant difference in temperature between streets oriented north-south versus east-west, heating and ventilation may have been more consistent in the current study site than in past studies, for instance because San Francisco is at a lower latitude and is less dense than European cities, and less dense than many Asian cities where variability with street orientation were observed (Jansson et al. 2007, Oliveira et al. 2011, Ng et al. 2012). Street orientation may still strongly affect surface temperature (Chudnovsky 2004; Golden and Kaloush 2006), however surface temperature contrasts are in imperfect proxy for overlying air temperature (Spronken-Smith and Oke 1998).

4.2 Park Cool Island Effect

Golden Gate Park showed a persistent and significant PCI. The magnitude of the mean PCI intensity of 1.1°C at 1.1 m under typical conditions was close to the average cooling effect of 0.94°C (CI 0.71-1.16°C) estimated by Bowler et al. (2010) from 26 sites

and 16 studies. This is perhaps surprising given the cool, windy ambient atmospheric conditions, however it may be explained by the exceptionally large size of Golden Gate Park. Chang et al. (2007) found parks greater than 3 ha in area were more likely to show a cooling effect based on 61 parks in Taipei City. Barradas (1991) found among parks ranging in size from 1.9 to 9.9 ha that larger parks tended to produce a greater cooling effect. Comparably sized parks are rare in the literature, however what evidence exists suggests that large parks tend to be at least a few degrees cooler than their surroundings near the surface. Jauregui (1990/1991) reports Chapultepec Park in Mexico City (500 ha) was 2-3°C cooler than the surrounding city during daytime traverses. Similar magnitudes of 2-3°C were found on a single nocturnal traverse through Central Park in New York City (341 ha) reported by Gaffin et al. (2008), however the authors noted from measurements above rooftop level that Central Park was cooler than its surroundings only at night.

The PCI was preserved for the most part in the entire vertical profile to 2.5 m. This was least true at the surface. In the forested site, the PCI was greatest near the surface due to the low rates of surface heating there, while the PCI was smallest near the surface over the short grass. This means the short grassy surface was a significant atmospheric heat source within the park, offset by cooling from surrounding taller vegetation.

Mean PCI was two times larger during the heat event than under typical conditions, affirming that PCI magnitude is directly related to temperature (Shashua-Bar and Hoffman 2000, Cohen 2012). These results confirm findings of Cohen et al. (2012) that with the atypical synoptic conditions that produce heat waves in coastal Mediterranean climates, as ocean cooling diminishes, park cooling becomes more

pronounced. This is significant since in the absence of a prominent sea breeze that regulates the temperatures to which an urban population is acclimated park cooling becomes an important in avoiding human health effects of abnormally high temperatures. Recent downscaling of global climate models to regional climates in California suggests that the frequency and duration of heat waves is likely to increase in coming decades, especially in coastal areas (Gershunov and Guirguis 2012). In particular as the climate warms and the scale of thermodynamic energy exchanges increases, larger continental high pressure systems capable of impacting weather across thousands of kilometers will occur with greater frequency, which will overwhelm the local onshore gradient in coastal areas (Gershunov and Guirguis 2012).

4.3 Role of Shade in Park Cooling

The correlation between shade, surface temperature, and air temperature above the surface illustrated in Figure 9 suggests shade plays a significant role in temperature variability overall, in both park and urban spaces. Shade is typically the reason why in forested areas, PCI peaks in the daytime (Cohen et al. 2012, Spronken-Smith and Oke 1998), although Potcher (2006) found that dense trees reduce nighttime advection and retain heat and relative humidity after dark, and thus can be a source of nocturnal discomfort under high heat conditions. Tall trees with wide canopies and limited understories may be most efficient for providing both daytime and nighttime cooling.

Shade contributes to park cooling by reducing the net energy budget where solar radiation is reflected or absorbed above the surface level. The cooling effects of shade

were available in the shaded portion of the open meadow shown in Figure 10 as well as under the tree canopies, demonstrating that the effect of shade persists even in open areas with greater exposure to advective and thermodynamic forces. The shadows that cooled half of the meadow shown in Figure 10 make strict associations between land cover types and park cooling more difficult.

The influence of shade on air temperatures is most strongly evidenced by the near surface gradient, which is shown in Figure 11. Sampled land cover areas with more shade tended to be cooler near the surface and exhibit a narrower range of temperatures overall.

4.4 Humidity as an indicator of Park Cooling

In semi-arid climates, increased water availability leads to increased evaporation, which cools the surrounding area by absorbing energy into the latent heat of evaporation (Ng et al. 2012). In the current study, the small number of observations during the elevated heat period limits any strong conclusions, however the trend suggest a strong relationship between small changes in absolute humidity and increases in PCI intensity, and furthermore suggests that the relationship is heightened by contrasts in absolute humidity in park areas the surrounding area. As illustrated by Spronken-Smith et al. (2000), while some of the increased water availability in urban parks is due to the relatively greater capacity for plants and soils to store ground water and precipitation, two other factors that contribute are (1) water inputs from irrigation in urban areas and (2) the contrast in temperature and humidity drives circulation from

the drier urban area. As warm air subsides above the park, sensible heat is converted to latent heat of evaporation, and the park cools. Where the park soil is water saturated, the effect is “thermostatic” because the process is limited by the available energy, not by water availability. Spronken-Smith et al. (2000) demonstrated that evaporation above an irrigated suburban park was 300% greater than evaporation in the surrounding area, while evaporation above a nearby irrigated rural area was 130% greater.

The temperature profile for Sharon Meadow in Figure 12 similarly demonstrates that irrigation can produce significant cooling by increasing the amount of available water in the park without increasing water availability in the surrounding area. Even as the surface heated over the course of the morning, the vertical temperature profile remained significantly lower compared to other sampled land cover areas. By contrast in Figure 13, fog condensation and limited sunlight throughout the morning produced a warmer profile in Sharon Meadow than in the surrounding city blocks.

Figure 14 demonstrates that absolute humidity contrasts between the park and surrounding city blocks are consistently associated with higher PCI values, under elevated heat conditions as well as under typical conditions. Chow et al. (2012) caution against using such findings to design a heat mitigation strategy around irrigation in parks, particularly in climates where water is relatively scarce, as the volume of water evaporated under such conditions may not be an efficient use of resources.

4.5 Park to Urban Gradient

Bowler et al. (2010) emphasized that park cooling, as a meaningful mitigation against urban heating, depends on whether park-cooled air travels outside the park. Shashua-Bar and Hoffman (2000) estimated the decay rate of cooling with distance from small parks in Tel Aviv, and an average decay rate of 0.231°C for every 10 m distance from the park, two orders of magnitude greater than the values recorded in Table 6. Shashua-Bar and Hoffman (2000) emphasize that the effect disappeared entirely beyond 100 m. Similarly, the gradients calculated in Table 6 disappeared within one block (500 m). This suggests that the horizontal extent of park cooling beyond park boundaries is site-specific, and may not vary with the size of the park as suggested by Jauregui 1990/1991 and Bowler et al. 2010, since Golden Gate Park is 422 ha and the park sites in Shashua-Bar and Hoffman (2000) ranged in size from 0.04 to 1.1 ha.

The extent of advective cooling from parks depends also on the geometry and orientation of the surrounding structures. Oliveira et al. (2011) reported some of the largest PCI magnitudes in the literature based on measurements from a courtyard park surrounded on all sides by tall buildings. The walls of the courtyard prevent the cooling from dissipating, thereby providing more immediate relief to park users and adjacent buildings, however the effect of park cooling becomes more localized where physical barriers prevent the pool of cool air from spreading across the surrounding urban fabric.

Past studies have suggested one park width downwind as a reasonable rule of thumb for the extent of a park cool island's effect on the adjacent land uses (Jauregui 1990/1991, Spronken Smith and Oke 1998). Based on empirical study, Ca et al. (1998)

estimate that in a strong wind, park breeze from a 35 ha park can go 1 km. However evidence from the current study suggests that the cooling benefit of parks exists primarily within the park, with limited impact beyond the boundaries. Furthermore, as demonstrated by Spronken-Smith et al. (2000), when the vapor pressure deficit decreases under maximum heat conditions, Golden Gate Park may be more efficient as an evaporation engine than as a cooling engine. Small-scale interventions such as tree plantings and green roofs may have more potential for mitigating urban heat not only by providing shade and evapotranspiration, but by disrupting the super-adiabatic lapse rates typical of urban spaces (Streiling and Matzarakis 2003).

5. Conclusions

The current study has explored the use of vertical temperature profiles as a means of understanding the characteristics of park cooling in Golden Gate Park in San Francisco, California. Results demonstrate that Golden Gate Park is persistently cooler than its urban surroundings 1.1 to 1.8°C under typical summer conditions, and 2.5 to 3.5°C during a heat event. The temperature of the surroundings varies with distance from the ocean by a gradient as strong as 1.9°C km⁻¹ along a 5 km park width. Park cooling increases with temperature and relative humidity inside the park. The impact of irrigation on cooling is greatest near the surface, as is temperature variability and sensitivity.

Using fine-wire thermocouples mounted at multiple heights demonstrated that different land cover areas have signature profiles. The shape of these profiles ranged from super-adiabatic to isothermal, governed primarily by patterns of sun and shade. Urban blocks with consistent height and width have similar vertical profiles, whereas park areas with different vegetation structures exhibit very different temperature structures in the vertical profile. Park cooling increases with elevated heat conditions brought on by changes in synoptic scale weather patterns, however the characteristic temperature structures persist.

The magnitude of park cooling is similar to results from warmer climates and milder onshore gradients, which may have to do with the significant size of the park. However the cooling effect of the park drops off as fast or faster than much smaller parks beyond the park boundary.

Future research should examine the relationship between temperature structure and cooling through urban greening on urban heat, particularly the impact of the change in temperature structure as indicated by the vertical profile induced by shade trees and green roofs.

6. Works Cited

- Barradas, V.L., 1991. Air temperature and humidity and human comfort index of some city parks of Mexico City. *International Journal of Biometeorology* 35(1): 24–28.
- Bowler, D. E., L. Buyung-Ali, T. M. Knight, and A. S. Pullin. 2010. Urban greening to cool towns and cities: A systematic review of the empirical evidence. *Landscape and Urban Planning* 97 (3):147–155.
- Ca, V. T., T. Asaeda, and E. M. Abu. 1998. Reductions in air conditioning energy caused by a nearby park. *Energy and Buildings* 29 (1):83–92.
- Cao, X., A. Onishi, J. Chen, and H. Imura. 2010. Quantifying the cool island intensity of urban parks using ASTER and IKONOS data. *Landscape and Urban Planning* 96 (4):224–231.
- Chang, C.-R., M.-H. Li, and S.-D. Chang. 2007. A preliminary study on the local cool-island intensity of Taipei city parks. *Landscape and Urban Planning* 80 (4):386–395.
- Chow, W. T. L., R. L. Pope, C. A. Martin, and A. J. Brazel. 2011. Observing and modeling the nocturnal park cool island of an arid city: horizontal and vertical impacts. *Theoretical and Applied Climatology* 103 (1-2):197–211.
- Chow, W. T. L., and A. J. Brazel. 2012. Assessing xeriscaping as a sustainable heat island mitigation approach for a desert city. *Building and Environment* 47 (0):170–181.
- Cohen, P., O. Potchter, and A. Matzarakis. 2012. Daily and seasonal climatic conditions of green urban open spaces in the Mediterranean climate and their impact on human comfort. *Building and Environment* 51:285–295.

- Eliasson, I., and H. Upmanis. 2000. Nocturnal Airflow from Urban Parks-Implications for City Ventilation. *Theoretical and Applied Climatology* 66 (1):95–107.
- Givoni, B. 1991. Impact of planted areas on urban environmental quality: A review. *Atmospheric Environment. Part B. Urban Atmosphere* 25 (3):289–299.
- Chudnovsky, A., E. Ben-Dor, and H. Saaroni. 2004. Diurnal thermal behavior of selected urban objects using remote sensing measurements. *Energy and Buildings* 36 (11):1063–1074.
- Gaffin, S. R., C. Rosenzweig, R. Khanbilvardi, L. Parshall, S. Mahani, H. Glickman, R. Goldberg, R. Blake, R. B. Slosberg, and D. Hillel. 2008. Variations in New York city's urban heat island strength over time and space. *Theoretical and Applied Climatology* 94 (1-2):1–11.
- Gershunov, A., and K. Guirguis. 2012. California heat waves in the present and future. *Geophysical Research Letters* 39 (18).
- Gomez, F., E. Gaja, and A. Reig. 1998. Vegetation and climatic changes in a city. *Ecological Engineering* 10:355–360.
- Hart, M. A., and D. J. Sailor. 2008. Quantifying the influence of land-use and surface characteristics on spatial variability in the urban heat island. *Theoretical and Applied Climatology* 95:397–406.
- Golden, J. S., and K. E. Kaloush. 2006. Mesoscale and microscale evaluation of surface pavement impacts on the urban heat island effects. *International Journal of Pavement Engineering* 7 (1):37–52.

- Grimmond CSB, Oke TR (1999) Heat storage in urban areas: Local-scale observations and evaluation of a simple model. *Journal of Applied Meteorology* 38: 922–940
- Heisler, G. M., and A. J. Brazel. 2010. The urban physical environment: Temperature and urban heat islands. *Urban Ecosystem Ecology* (urbanecosysteme):29–56.
- Jansson, C., P.-E. Jansson, and D. Gustafsson. 2007. Near surface climate in an urban vegetated park and its surroundings. *Theoretical and Applied Climatology* 89 (3-4):185–193.
- Jauregui, E. 1990/1991. Influence of a large urban park on temperature and convective precipitation in a tropical city. *Energy and Buildings* 15:457–463.
- Lindén, J. 2011. Nocturnal Cool Island in the Sahelian city of Ouagadougou, Burkina Faso. *International Journal of Climatology* 31 (4):605–620.
- Murphy, D. J. et al. 2011. The relationship between land cover and the urban heat island in northeastern Puerto Rico. *International Journal of Climatology* 31:1222–1239.
- Lu, J., C. Li, Y. Yang, X. Zhang, and M. Jin. 2012. Quantitative evaluation of urban park cool island factors in mountain city. *Journal of Central South University* 19 (6):1657–1662.
- Oke, T. R. 1987. *Boundary layer climates*. 2nd Ed. Routledge.
- Oliveira, S., H. Andrade, and T. Vaz. 2011. The cooling effect of green spaces as a contribution to the mitigation of urban heat: A case study in Lisbon. *Building and Environment* 46:2186–2194.

- Potchter, O., P. Cohen, and A. Bitan. 2006. Climatic behavior of various urban parks during hot and humid summer in the Mediterranean city of Tel Aviv, Israel. *International Journal of Climatology* 26 (12):1695–1711.
- Rosenfeld, A. H. et al. 1995. Mitigation of urban heat islands: materials, utility programs, updates. *Energy and Buildings* 22 (3):255–265.
- Shashua-Bar, L., and M. E. Hoffman. 2000. Vegetation as a climatic component in the design of an urban street: An empirical model for predicting the cooling effect of urban green areas with trees. *Energy and Buildings* 31 (3):221–235.
- Saaroni, H., E. Ben-Dor, A. Bitan, and O. Potchter. 2000. Spatial distribution and microscale characteristics of the urban heat island in Tel-Aviv, Israel. *Landscape and Urban Planning* 48:1–18.
- Souch, C., and S. Grimmond. 2006. Applied climatology: urban climate. *Progress in Physical Geography* 30 (2):270–279.
- Spronken-Smith, R. A., and T. R. Oke. 1998. The thermal regime of urban parks in two cities with different summer climates. *International Journal of Remote Sensing* 19 (11):2085–2104.
- Spronken-Smith, R. A., T. R. Oke, and W. P. Lowry. 2000. Advection and the surface energy balance across an irrigated urban park. *International Journal of Climatology* 20 (9):1033–1047.
- Sun, C.-Y. 2011. A street thermal environment study in summer by the mobile transect technique. *Theoretical and Applied Climatology* 106:433–442.

- Yokobori, T., and S. Ohta. 2009. Effect of land cover on air temperatures involved in the development of an intra-urban heat island. *Climate Research* 39:61–73.
- Streiling, S., and A. Matzarakis. 2003. Influence of single and small clusters of trees on the bioclimate of a city: a case study. *Journal of Arboriculture* 29 (6):309–316.
- Upmanis, H., I. Eliasson, and S. Lindqvist. 1998. The influence of green areas on nocturnal temperatures in a high latitude city (Göteborg, Sweden). *International Journal of Climatology* 18 (6):681–700.
- Yokohari, M., R. D. Brown, Y. Kato, and H. Moriyama. 1997. Effects of paddy fields on summertime air and surface temperatures in urban fringe areas of Tokyo, Japan. *Landscape and Urban Planning* 38 (1-2):1–11.
- Yu, C., and W. N. Hien. 2006. Thermal benefits of city parks. *Energy and Buildings* 38 (2):105–120.
- Voogt, J. A., and T. R. Oke. 1997. Complete urban surface temperatures. *Journal of Applied Meteorology* 36 (9):1117.
- Wong, N. H., and C. Yu. 2005. Study of green areas and urban heat island in a tropical city. *Habitat International* 29 (3):547–558.